Hindawi Publishing Corporation
International Journal of Photoenergy
Volume 2008, Article ID 185479, 5 pages
doi:10.1155/2008/185479

Research Article

Photo-Oxidation of Water Using Nanocrystalline Tungsten Oxide under Visible Light

J. W. J. Hamilton, J. A. Byrne, P. S. M. Dunlop, and N. M. D. Brown

Nanotechnology and Integrated BioEngineering Centre, University of Ulster, Jordanstown, County Antrim BT37 0QB, Northern Ireland, UK

Correspondence should be addressed to J. W. J. Hamilton, jwj.hamilton@ulster.ac.uk

Received 21 August 2007; Accepted 24 January 2008

Recommended by Ignazio Bellobono

The photoelectrolysis of water to yield hydrogen and oxygen using visible light has enormous potential for solar energy harvesting if suitable photoelectrode materials can be developed. Few of the materials with a band gap suitable for visible light activation have the necessary band-edge potentials or photochemical stability to be suitable candidates. Tungsten oxide (E_{bg} 2.8 eV) is a good candidate with absorption up to $\lambda \approx 440$ nm and known photochemical stability. Thin films of tungsten oxide were prepared using an electrolytic route from peroxo-tungsten precursors. The tungsten oxide thin films were characterised by FESEM, Auger electron spectroscopy, and photoelectrochemical methods. The magnitude of the photocurrent response of the films under solar simulated irradiation showed a dependence on precursor used in the film preparation, with a comparatively lower response for samples containing impurities. The photocurrent response spectrum of the tungsten oxide films was more favourable than that recorded for titanium dioxide (TiO_2) thin films. The WO_3 photocurrent response was of equivalent magnitude but shifted into the visible region of the spectrum, as compared to that of the TiO_2.

1. INTRODUCTION

In 1969, Fujishima and Honda reported the photoelectrolysis of water using single crystal rutile titanium dioxide under UV irradiation [1]. Since then, the use of titanium dioxide photocatalysis for environmental remediation of air and water has been intensively explored and is well documented [2]. However, TiO_2 is a wide band gap semiconductor (anatase, $E_{bg} = 3.2$ eV) and absorbs light of wavelengths ≤ 387 nm. Therefore, only a small proportion of the solar energy spectrum (<5%) can be utilised. In order to facilitate further advancement in the field of semiconductor photocatalysis using solar energy, researchers are looking at other narrow band materials which absorb in the visible region of the solar spectrum. Unfortunately, visible light absorbing semiconductors are either unstable in contact with water or do not have the necessary band edge potentials necessary for the desired electrochemistry. Tungsten oxide has a reported band gap of 2.6 to 2.8 eV [3] with band edges located at $E_{cb} - 0.3$ V and $E_{VB} + 2.4$ V at pH 7 [4], making it a possible candidate material for the photoelectrolysis of water using visible light. The preparation of WO_3 is relatively well explored and its use for the photoelectrolysis of water has also been reported [5–14]. Additionally, doped WO_3 and multilayered photocatalysts incorporating WO_3 have been investigated [14–16].

However, the majority of publications concerning preparation and characterisation of WO_3 have produced thin films by sol-gel synthesis. The use of sol-gel synthesis with tungsten alkoxides has been reported to produce porous films with excessive carbon impurities [17]. Zhitomirsky et al. previously reported that manymetal oxides, in which the metal of parent compound formed polyperoxoacids on reaction with hydrogen peroxide, could be electrolytically deposited as oxide thin films [18, 19]. Although they did not specifically report the electrolytic deposition of tungsten oxide, other workers have used such a method to produce electrochromic materials [20].

In this work, peroxotungstic acids were produced from a range of precursors. Previous literature [21] has reported the production of peroxotungstates from otherwise highly stable

carbide under the action of H_2O_2. In this work tungsten oxide, tungstic acid, and tungsten dodecaphosphate were used as precursors for the production of polyperoxoacids of tungsten by digestion in H_2O_2, from which thin films were prepared. Films were characterised by FESEM, AES, and photoelectrochemical methods with comparison to sol-gel TiO_2 films as a reference standard.

2. EXPERIMENTAL

Tungsten oxide thin films were produced via a modified electrolytic route. Peroxoprecursors were prepared by dissolving 2.5 g of tungsten oxide, tungstic acid (Sigma-Aldrich Company Ltd., The Old Brickyard, New Road, Gillingham, Dorset SP8 4XT), or tungsten dodecaphosphate (BDH) in 15 cm^3 of H_2O_2 (30%) and 10 cm^3 H_2O. The precursor slurries were heated at 70°C for 10 minutes to dissolve all the powder starting material, generating a viscous yellow peroxotungsten precursor. During the powder digestion reactions, all tungsten precursors exchange their ligands for peroxo ligands. The peroxotungsten species produced by reaction of tungsten compounds with hydrogen peroxide are a complex mixture. These include monotungstate species $WO_2(O_2)_2^{2-}$, $WO(OH)(O_2)_2^{2-}$, bitungstate species $W_2O_3(O_2)_4^{2-}$, and more complicated species [22]. For this reaction scheme, only the simplest species produced in the initial reaction is considered (see (1)). During the extended heating, tungsten species undergo condensation/polymerisation reactions, similar to those of a sol-gel precursor (see (2)) [22]. These condensation reactions form complex chains and other structures of repeating peroxotungstate units resulting in an increase in the viscosity of the solution:

$$W - L_X + 3H_2O_2 \longrightarrow WO_2(O_2)_2^{2-} + 6H^+ + L_X^{Y-}, \quad (1)$$

$$2WO_2(O_2)_2^{2-} + 2H^+ \longrightarrow W_2O_3(O_2)_2^{2-} + H_2O. \quad (2)$$

WO_3 films were formed by electrochemical oxidation of the peroxotungstates on tungsten foil and gas evolution were observed at the anode during film formation. The presumed anodic half cell reaction is given in (3):

$$2WO_2(O_2)_2^{2-} \longrightarrow 2WO_3 + 3O_2 + 4e^-. \quad (3)$$

For AES analysis, films were deposited on titanium metal foil to eliminate the tungsten signal of the substrate from interfering. Anodic electrolytic deposition was carried out under a constant current of 10 mA for 200 seconds on 1.5 cm^{-2} tungsten foil coupons. The deposition time was reduced to 60 seconds on titanium foil samples (1.5 cm^2), for elucidation of the growth mechanism. Constant current anodic deposition was used as this gave more reproducible films in terms of microstructure. After electrolytic treatment, the films were washed with distilled water and dried in air. The tungsten foil samples were annealed at 500°C for 1 hour with a temperature ramp of 5°C min^{-1}.

Titanium dioxide thin films were prepared by a sol-gel route adapted from Murakami et al. [23]. Butan-1-ol (10 cm^3) was added to a round bottom flask, which was placed on a balance and the balance rezeroed. Using a syringe, titanium butoxide was removed from its sealed bottle via the rubber septum. With the tip of the syringe immersed in the butanol, 0.377 g of butoxide was added to the flask. A magnetic stirring bar was added and the flask was sealed with Parafilm™. The round-bottomed flask was then transferred to a stirrer. Ammonium acetate (0.0973 g) was dissolved in 0.2 cm^3 of distilled water in a micro beaker. The contents of the beaker were then washed into a clean, dry, separating funnel with 15 cm^3 of butan-1-ol and shaken to mix the two solvents. The Parafilm™ was then removed from the neck of the round-bottomed flask and the dropping funnel containing water, solvent, and salt catalyst was attached at the quick fit junction. The contents of the dropping funnel were added dropwise under constant stirring. The reaction solution was finally aged for 1 hour before dip coating (withdrawal rate 6 mm s^{-1}).

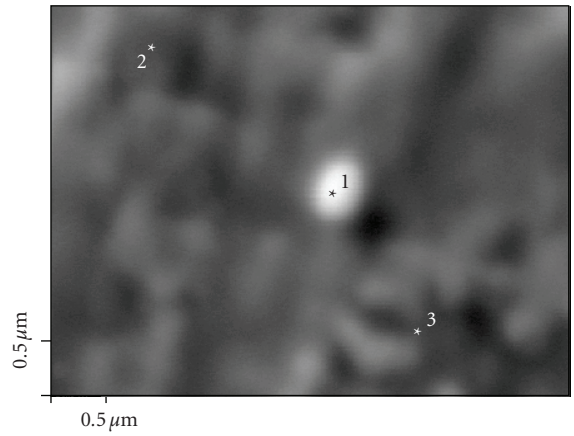

Figure 1: SEM showing WO_3 film and locations selected for AES analysis.

Tungsten oxide samples deposited on titanium foil were imaged by field emission SEM and elemental analysis was carried out by Auger electron spectroscopy (Perkin-Elmer Φ 660) with vacuum of 10^{-6} Torr with electrons accelerated from a field emission source at 4 kV accelerating voltage to give a beam current of ~2 μA.

For electrochemical measurements, electrical contacts were made by attaching copper wire with conductive silver epoxy (Circuit Works, Chemtronics) to the back of the foil (cleaned to remove oxide) and insulated using with negative photoresist (KPR resist, Casio Chemicals) to give an exposed oxide area of 1 cm^2.

Electrochemical characterisation of samples was performed under potentiostatic control (Autolab PGSTAT30) in a one-compartment glass cell containing a quartz window with a platinum basket counter electrode and a saturated calomel electrode (SCE) reference electrode. All potentials are reported versus SCE. The supporting electrolyte was 0.1 M $LiClO_4$ and irradiation was provided by a 1 kW Xe arc lamp (ss1000 Spears Robinson) with an AM1 filter to simulate solar conditions. For monochromatic irradiation

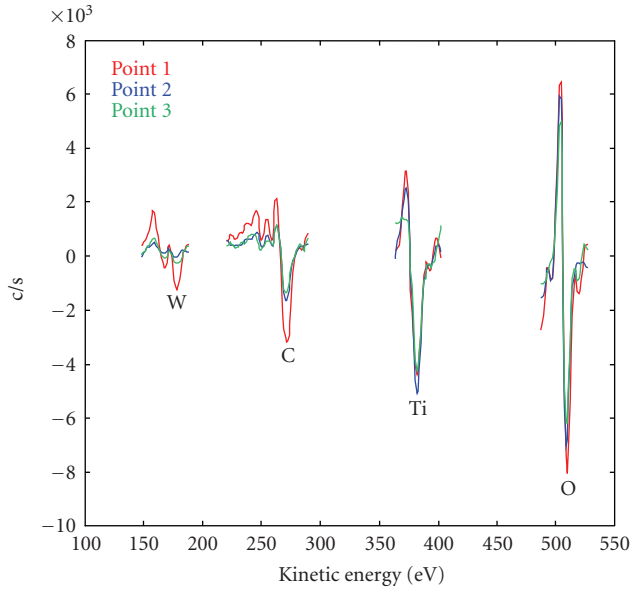

Figure 2: AES spectra from points selected in Figure 1.

Table 1: Elemental by AES analysis of points in SEM (Figure 1).

%	C	O	Ti	W
Point 1	33.24	32.51	19.13	15.12
Point 2	25.26	42.43	28.10	4.20
Point 3	25.83	41.87	24.05	8.26

experiments, a monochromator (GM252, set for 10 nm band pass) was positioned between the source (unfiltered) and the photoelectrochemical cell. Linear sweep voltammograms were measured scanning from −1.0 V to +1.5 V at a scan rate 10 mV s^{-1}. The current-time response was measured at +1.0 V using chopped illumination (chopper Uniblitz vmm-t1, Vincent Associates). The cell temperature was maintained at 25°C ± 2°C.

3. RESULTS AND DISCUSSION

To examine the electrolytic growth of tungsten oxide, samples were prepared on titanium foil to ensure that the WO_3 thin film grown by the electrolytic process was not simply due to anodisation of the tungsten foil itself. FESEM analysis showed that the films were nonuniform with more WO_3 deposition around the edges of the electrode. The uneven deposition observed is not uncommon for electrodeposited films and is due to edge effects.

The surface of the sample showed grain-like structures (Figure 1). Features were selected for elemental analysis (Figure 1, points 1–3) using AES and the corresponding spectra are given in Figure 2.

The surface showed significant amounts of tungsten and oxygen in addition to the titanium of the underlying support electrode. The concentration of elements in the selected points is given in Table 1.

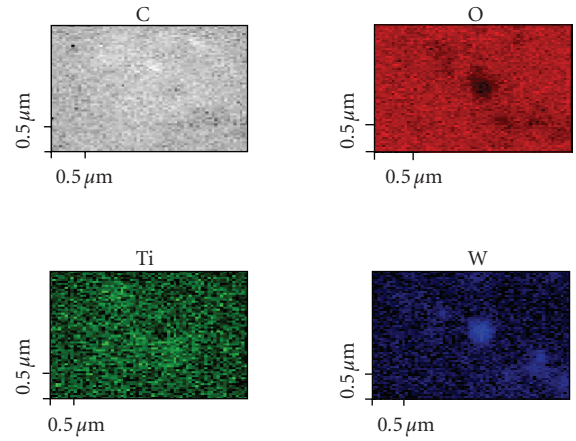

Figure 3: Colour coded SEM images showing the elemental distribution on the surface.

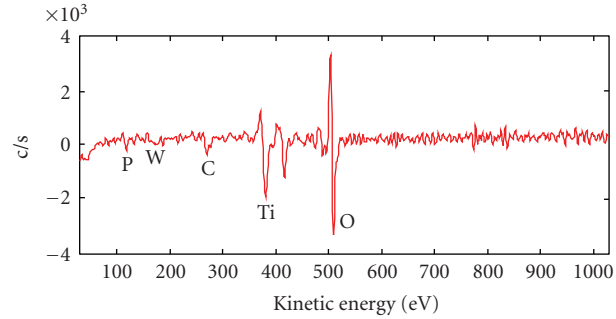

Figure 4: AES spectrum for the WO_3 film prepared from the dodecaphosphate precursor showing a small signal due to phosphorous contamination.

This analysis showed the WO_3 to have grown in islands with the highest concentration of tungsten measured in the grain-like features (point 1 in Figure 1 and Table 1). This is also shown in elemental colour mapped SEM images produced using AES (Figure 3). In the colour mapped images, the lighter colours indicate higher concentrations of the element and darker colours representing lower concentrations, and black indicating the absence of the element.

Imaging of samples produced from other precursors (tungsten oxide, tungsten dodecaphosphate) showed a similar growth with islands of material building up preferentially at the edges. The samples produced from the tungsten dodecaphosphate precursor contained a small quantity of phosphorus (see Figure 4).

The photoelectrochemical characterisation of the films using LSV showed a typical *n*-type response with no anodic current observed in the dark and photocurrent a potentials more positive than 0.0 V (Figure 5). The films produced from the tungstic acid precursor gave the highest relative photocurrent.

Comparison of photocurrent densities produced from WO_3 thin films and TiO_2 at +1.0 V are given in Table 2. The WO_3 films had a higher photocurrent density than that of

Table 2: A comparison of photocurrent densities produced under solar simulated conditions at +1.0V.

Material	Tungsten oxide			Titanium dioxide via sol-gel route
Precursor	Tungsten oxide	Tungstic acid	Tungsten dodeca phosphate	
Photocurrent (mA cm^{-1})	0.674	0.974	0.134	0.266

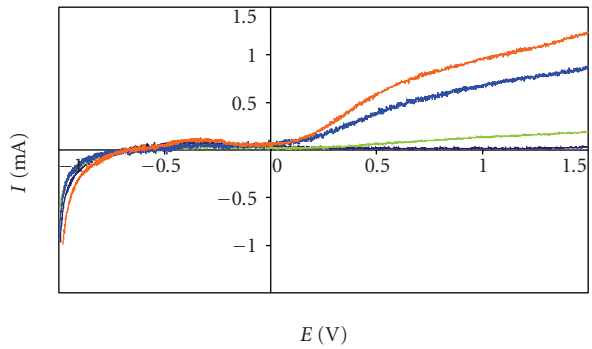

Figure 5: Comparison of photocurrent response of WO_3 film electrodes prepared from different precursors, that is, tungsten dodecophosphate (green line), tungsten oxide (blue line), tungstic acid (red line) and with dark current response (dark blue).

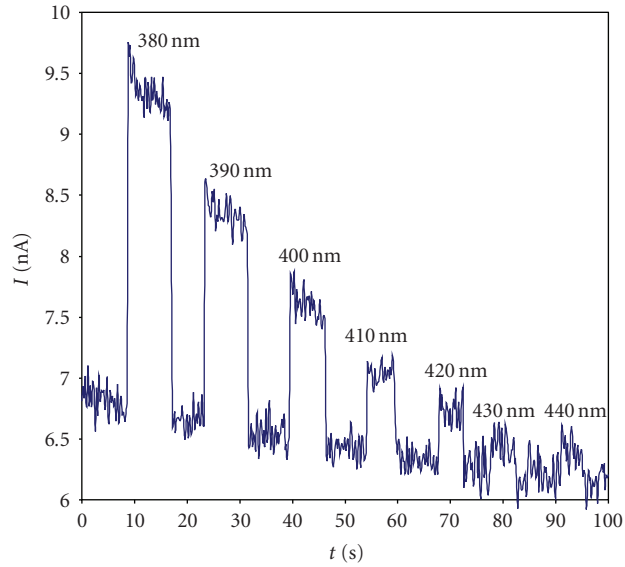

Figure 6: Photocurrent response of WO_3 under monochromatic irradiation (bandwidth 10 nm).

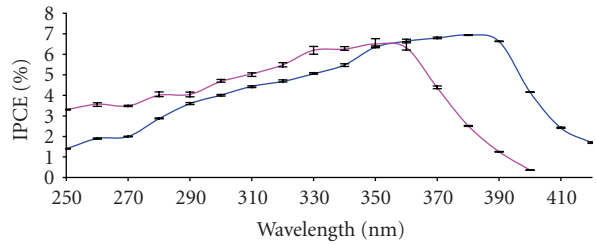

Figure 7: Comparison of the %IPCE of TiO_2 (pink line) and WO_3 (blue line) as a function of wavelength.

the TiO_2 thin films prepared via a sol-gel route under solar simulated irradiation.

Figure 6 shows the current-time response of the tungstic acid derived WO_3 film under monochromatic irradiation showing a small photocurrent response in the visible ($\lambda >$ 420 nm—not normalised to monochromator output).

Using light intensity measurements the photocurrent produced under monochromatic irradiation was used to calculate incident photon to current conversion efficiency

$$\%\text{IPCE} = \left(\frac{J}{I_0 F}\right) \times 100, \tag{4}$$

where J is the photocurrent density, I_0 is the incident light intensity (band pass 10 nm), and F is Faraday's constant. A comparison of the photon conversion efficiency between WO_3 and TiO_2 thin films is given in Figure 7 which shows both materials exhibited ~7% efficiency at peak wavelengths 355 nm and 380 nm, respectively.

The response spectrum of WO_3 extended to longer wavelengths into the visible region of the spectrum.

4. CONCLUSIONS

Surface characterisation of WO_3 films prepared from peroxo-polytungstate precursors confirmed the growth of WO_3. Photoelectrochemical measurements under simulated solar irradiation showed that the WO_3 films behaved as n-type semiconductors producing anodic current only under irradiation. Comparison of samples produced from different precursors showed that the films prepared using the tungstic acid precursor gave the highest relative photocurrent. The lower photocurrent from the films prepared from tungsten dodecaphosphate could be attributed to phosphorus impurities in the film. The WO_3 films gave a higher photocurrent response under simulated solar irradiation compared to sol-gel derived TiO_2 films. Photocurrent response spectra measured under monochromatic irradiation showed similar peak efficiency (~7%) at 355 nm for TiO_2 and 380 nm for WO_3. However, the photocurrent spectral response for the WO_3 films was red-shifted into the visible region of the spectrum. Further work is needed to determine the O_2 and H_2 yield under prolonged, simulated solar irradiation.

ACKNOWLEDGMENT

The authors would like to thank Dr. Naiya Cui for help with AES analysis.

REFERENCES

[1] A. Fujishima and K. Honda, "Electrochemical photolysis of water at a semiconductor electrode," *Nature*, vol. 238, no. 5358, pp. 37–38, 1972.

[2] M. Kaneko and I. Okura, *Photocatalysis: Science and Technology*, Springer, Berlin, Germany, 2002.

[3] C. G. Granqvist, *Handbook of Inorganic Electrochromic Materials*, chapter 2, Elsevier, Amsterdam, The Netherlands, 1995.

[4] A. Mills and S. Le Hunte, "An overview of semiconductor photocatalysis," *Journal of Photochemistry and Photobiology A*, vol. 108, no. 1, pp. 1–35, 1997.

[5] J. R. Darwent and A. Mills, "Photooxidation of water sensitized by WO_3 powder," *Journal of Chemical Society, Faraday Transactions*, vol. 78, no. 2, pp. 359–367, 1982.

[6] G. R. Bamwenda and H. Arakawa, "The photoinduced evolution of O_2 and H_2 from a WO_3 aqueous suspension in the presence of Ce^{4+}/Ce^{3+}," *Solar Energy Materials and Solar Cells*, vol. 70, no. 1, pp. 1–14, 2001.

[7] H. Kominami, K. Yabutani, T. Yamamoto, Y. Kara, and B. Ohtani, "Synthesis of highly active tungsten(VI) oxide photocatalysts for oxygen evolution by hydrothermal treatment of aqueous tungstic acid solutions," *Journal of Materials Chemistry*, vol. 11, no. 12, pp. 3222–3227, 2001.

[8] K. Sayama, R. Yoshida, H. Kusama, K. Okabe, Y. Abe, and H. Arakawa, "Photocatalytic decomposition of water into H_2 and O_2 by a two-step photoexcitation reaction using a WO_3 suspension catalyst and an Fe^{3+}/Fe^{2+} redox system," *Chemical Physics Letters*, vol. 277, no. 4, pp. 387–391, 1997.

[9] J. Desilvestro and M. Neumann-Spallart, "Photoredox reactions on semiconductors at open circuit. Reduction of Fe^{3+} on WO_3 electrodes and particle suspensions," *Journal of Physical Chemistry*, vol. 89, no. 17, pp. 3684–3689, 1985.

[10] P. Maruthamuthu and M. Ashokkumar, "Hydrogen generation using Cu(II)/WO_3 and oxalic-acid by visible-light," *International Journal of Hydrogen Energy*, vol. 13, no. 11, pp. 677–680, 1988.

[11] C. Santato, M. Ulmann, and J. Augustynski, "Enhanced visible light conversion efficiency using nanocrystalline WO_3 films," *Advanced Materials*, vol. 13, no. 7, pp. 511–514, 2001.

[12] C. Santato, M. Ulmann, and J. Àugustynski, "Photoelectrochemical properties of nanostructured tungsten trioxide films," *Journal of Physical Chemistry B*, vol. 105, no. 5, pp. 936–940, 2001.

[13] G. R. Bamwenda, T. Uesigi, Y. Abe, K. Sayama, and H. Arakawa, "The photocatalytic oxidation of water to O_2 over pure CeO_2, WO_3, and TiO_2 using Fe^{3+} and Ce^{4+} as electron acceptors," *Applied Catalysis A*, vol. 205, no. 1-2, pp. 117–128, 2001.

[14] T. Ohno, F. Tanigawa, K. Fujihara, S. Izumi, and M. Matsumura, "Photocatalytic oxidation of water on TiO_2-coated WO_3 particles by visible light using Iron(III) ions as electron acceptor," *Journal of Photochemistry and Photobiology A*, vol. 118, no. 1, pp. 41–44, 1998.

[15] D. W. Hwang, J. Kim, T. J. Park, and J. S. Lee, "Mg-doped WO_3 as a novel photocatalyst for visible light-induced water splitting," *Catalysis Letters*, vol. 80, no. 1-2, pp. 53–57, 2002.

[16] M. Ashokkumar and P. Maruthamuthu, "Preparation and characterization of doped WO_3 photocatalyst powders," *Journal of Materials Science*, vol. 24, no. 6, pp. 2135–2139, 1989.

[17] J. M. Bell, I. L. Skryabin, and A. J. Koplick, "Large area electrochromic films—preparation and performance," *Solar Energy Materials and Solar Cells*, vol. 68, no. 3-4, pp. 239–247, 2001.

[18] I. Zhitomirsky, L. Galor, A. Kohn, and H. W. Henicke, "Electrodeposition of ceramic films from nonaqueous and mixed-solutions," *Journal of Materials Science*, vol. 30, no. 20, pp. 3307–5312, 1995.

[19] I. Zhitomirsky, "Electrolytic deposition of oxide films in the presence of hydrogen peroxide," *Journal of the European Ceramic Society*, vol. 19, no. 15, pp. 2581–2587, 1999.

[20] A. Guerfi and L. H. Dao, "Electrochromic molybdenum oxide thin films prepared by electrodeposition," *Journal of the Electrochemical Society*, vol. 136, no. 8, pp. 2435–2436, 1989.

[21] T. Kudo, H. Okamoto, K. Matsumoto, and Y. Sasaki, "Peroxopolytungstic acids synthesized by direct reaction of tungsten or tungsten carbide with hydrogen-peroxide," *Inorganica Chimica Acta*, vol. 111, no. 2, pp. 27–28, 1986.

[22] H. Nakajima, T. Kudo, and N. Mizuno, "Reaction of metal, carbide, and nitride of tungsten with hydrogen peroxide characterized by ^{183}W nuclear magnetic resonance and raman spectroscopy," *Chemistry of Materials*, vol. 11, no. 3, pp. 691–697, 1999.

[23] Y. Murakami, T. Matsumoto, and Y. Takasu, "Salt catalysts containing basic anions and acidic cations for the sol-gel process of titanium alkoxide: controlling the kinetics and dimensionality of the resultant titanium oxide," *Journal of Physical Chemistry B*, vol. 103, no. 11, pp. 1836–1840, 1999.